Novel Thermotropic Liquid Crystalline and Redox-Active Complexes of Ionically Self-Assembled Poly(ferrocenylsilane) and Dendritic Amphiphiles

Zhiyu Cheng,[†] Biye Ren,* Dongli Zhao, Xinxing Liu, and Zhen Tong*

Research Institute of Materials Science, South China University of Technology, Guangzhou 510640, China

Received January 30, 2009; Revised Manuscript Received February 23, 2009

ABSTRACT: A series of novel polyelectrolyte-amphiphilie complexes were prepared by ionic self-assembly of cationic linear poly(ferrocenylsilane) (PFS) of $[Fe(\eta\text{-}C_5H_4)_2SiMe(OCH_2CH_2NMe_3I)]_n$ (**PFS**) with anionic dendrons of 3,4,5-tris(*n*-alkan-1-yloxy)benzoic acid [**(3,4,5)*n*G1-COOK**, $n = 12, 14, 16$, where n was the number of carbon atoms in the alkyl tail]. These complexes **PFS-(3,4,5)*n*G1** ($n = 12, 14, 16$) were characterized with XRD, FTIR, TG, DSC, cyclic voltammetry (CV), and polarized optical microscope (POM). XRD profiles indicated the presence of the crystalline phase in the complexes resulted from the dendritic amphiphiles, which formed the end-to-end bilayer lamellar structure with the long period $d = 4.84$, 5.34, and 5.76 nm for $n = 12$, 14, and 16, respectively. With increasing the length of amphiphile alkyl tails, the stacking order was improved. The ionic thermotropic liquid crystalline state was obtained from these **PFS-(3,4,5)*n*G1** complexes at temperature above the melting point of the dendron crystal. CV measurements indicated that these **PFS-(3,4,5)*n*G1** complexes exhibited a good reversible redox process. Our work provides for the first time a simply and facile approach to fabricate redox-active PFS polymers with ionic thermotropic liquid crystalline phase by the ionic self-assembly.

1. Introduction

The technique of ionic self-assembly, i.e., the coupling of oppositely charged building blocks by electrostatic attraction is a powerful tool to create new nanostructural and functional materials.[1] Considerable attemption has been made to the ionically self-assembled polyelectrolyte-amphiphile complexes (PAC) in the past decade due to their facile preparation, interesting properties, and various nanostructures, such as lamella, rodlike, column, and so on.[2−21] The dendritic amphiphile has the advantage of abundant structures of the side chains over conventional amphiphiles only with single or doubl tails, hence, the dendritic amphiphile as an alternative building block, provides a new foundation for designing novel polymer−amphiphile complexes. However, a few studies on the polymer-dendritic amphiphile complexes have been reported up to now.[18−26] Recently, Beginn and coworks prepared the ionic complex of poly(4-vinylpyridine) and mesognic wedge-shaped sulfonic acid.[23] They found that the complex was in a lamella phase at low degree of substitution, while a hexagonal columnar phase was observed at binding degree of 80 mol % and higher. In our previous work, the polymer−amphiphilic dendron complexes were prepared by ionic binding of trisubstituted benzoic acid dendrons on linear poly(ethyleneimine) (*l*PEI) or poly(allylamine hydrochloride) (PAH) and two mesomorphous structures were observed from the complexes: Lamella for the *l*PEI series and hexagonal column for the PAH series were formed irrespective of the chemical structure and alkyl tail length ($n \leq 12$) of the dendrons.[25]

Many efforts have been devoted to design new functional PACs for special applications by introducing functional building blocks in recent years.[9−13,27] One approach is to utilize functional polyelectrolytes. For example, binding surfactants on the conjugated polyelectrolytes, such as cationic poly(*p*-phenylene) (PPP),[11] anionic poly(1,4-phenyleneethynylene carboxylate) (PPE),[27] and poly(2,5-methoxypropyloxy sulfonate phenylene vinylene) (MPS-PPV),[10] tuned the optical and electronic properties of the component polymers. The merit of this simple approach is that complex properties can be adjusted by changing the nature of amphiphiles without synthesizing new polymers.

Water-soluble poly(ferrocenylsilane) (PFS), belonging to the rare class of the main-chain organometallic polyelectrolyte, is particularly attractive because it combines the unique property of PFS with the processability of polyelectrolytes.[28−36] For example, Hempenius et al.[34,35] found that these new main-chain organometallic polyelectrolytes can be utilized in the layer-by-layer assembly to fabricate ultrathin electroactive films useful in the electrode modification, electrocatalysis, electrochromism, and nano- and microlithography.[32] However, there is no report on water-soluble PFS electrostatically binding with oppositely charged amphiphiles, especially amphiphilic dendrons to form new complexes. At the same time, a few study concerned the thermotropic liquid-crystal of PFS.[37] We are wondering whether the PFS−dendron complex exhibits some novel structure and properties.

In the present work, ionic complexes of PFS polyelectrolytes $[Fe(\eta\text{-}C_5H_4)_2SiMe(OCH_2CH_2NMe_3I)]_n$ with trisubstributed benzoic acid dendrons, i.e., potassium salts of 3,4,5-tris(*n*-alkan-1-yloxy)benzoic acid [**(3,4,5)*n*G1-COOK**, $n = 12, 14, 16$, where n was the number of carbon atoms in the alkyl tail], were prepared (Scheme 1). These ionic complexes were investigated with X-ray diffraction (XRD), thermogravimetry (TG), differential scanning calorimetry (DSC), polarized optical microscope (POM), and cyclic voltammetry (CV).

2. Experimental Section

Materials. Methyl 3,4,5-trihydroxybenzoate (Aldrich, 98%) was used as received. 1-Bromododecane (98%), 1-bromotetradecane (98%), and 1-bromohexadecane (98%) from Yancheng Longsheng Fine Chemical Factory, China were distilled before use. Other reagents, such as ether, tetrahydrofuran (THF) and *N,N′*-dimethylformamide (DMF), were all analysis grade chemicals and freshly distilled prior to use. Water used for solutions was twice distilled. The trisubstituted benzoic acid dendrons, 3,4,5-tris(*n*-alkan-1-

* Corresponding authors. Telephone: (86)-20-87112886. Fax: (86)-20-87110273. E-mail: mcbyren@scut.edu.cn (B.R.); mcztong@scut.edu.cn (Z.T.).

[†] Present address: School of Materials Science and Technology, Wuhan Institute of Technology, Wuhan 430073, China.

10.1021/ma900207e CCC: $40.75
Published on Web 03/13/2009

Scheme 1

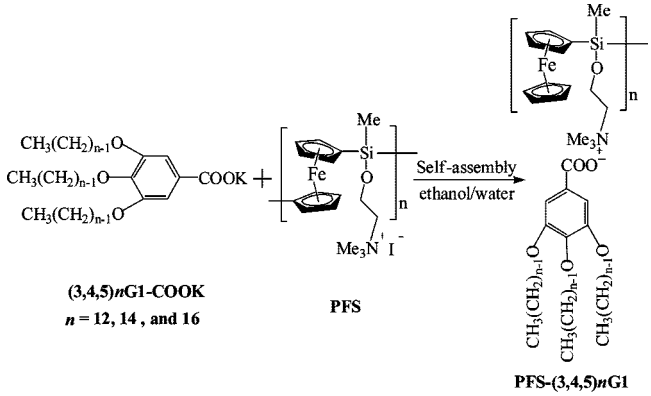

yloxy)- benzoic acid [**(3,4,5)*n*G1-COOH**, n = 12, 14, and 16], and their corresponding potassium salts (**(3,4,5)*n*G1-COOK**) were synthesized following the method reported by Percec et al. (Scheme 2).[25,38,39] Cationic poly(ferrocenylsilanes) [Fe(η-C_5H_4)$_2$SiMe-($OCH_2CH_2NMe_3I$)]$_n$ (PFS) was polymerized according to the documented procedure of Manners' group (Scheme 3).[28]

3,4,5-Tris(*n*-dodecan-1-yloxy)benzoic Acid [(3,4,5)12G1-COOH]. ^{1}H NMR ($CDCl_3$, TMS, δ, ppm): 0.88 (t, 9H, $-CH_3$), 1.28 (m, 48H, $-(CH_2)_8-$), 1.47 (m, 6H, $-CH_2-CH_2-CH_2-O-$Ar), 1.79 (m, 6H, $-CH_2-CH_2-O-$Ar), 4.02 (m, 6H, $-CH_2-O-$Ar), 7.32 (s, 2H, $-ArH_2-CO_2H$). Anal. Calcd for $C_{43}H_{78}O_5$: C, 76.50; H, 11.65. Found: C, 76.54; H, 11.72.

3,4,5-Tris(*n*-tetradecan-1-yloxy)benzoic Acid [(3,4, 5)14G1-COOH]. ^{1}H NMR ($CDCl_3$): 0.88 (t, 9H, $-CH_3$), 1.28 (m, 60H, -(CH_2)$_{10}$-), 1.47 (m, 6H, -CH_2-CH_2-CH_2-O-Ar), 1.79 (m, 6H, -CH_2-CH_2-O-Ar), 4.02 (m, 6H, -CH_2-O-Ar), 7.33 (s, 2H, -ArH_2-CO_2H). Anal. Calcd for $C_{49}H_{90}O_5$: C, 77.52; H, 11.95 and found: C, 77.58; H, 12.13.

3,4,5-Tris(*n*-hexadecan-1-yloxy)-benzoic acid [(3,4, 5)16G1-COOH]. ^{1}H NMR ($CDCl_3$): 0.88 (t, 9H, -CH_3), 1.28 (m, 72H, $-(CH_2)_{12}-$), 1.47 (m, 6H, $-CH_2-CH_2-CH_2-O-$Ar), 1.79 (m, 6H, $-CH_2-CH_2-O-$Ar), 4.02 (m, 6H, $-CH_2-O-$Ar), 7.33 (s, 2H, $-ArH_2-CO_2H$). Anal. Calcd for $C_{55}H_{102}O_5$: C, 78.32; H, 12.19. Found: C, 78.34; H, 12.25.

[Fe(η-C_5H_4)$_2$SiMe($OCH_2CH_2NMe_3I$)]$_n$ (PFS). ^{1}H NMR (DMF-d_7): 0.78 (s, 3H, Si$-CH_3$), 3.45 (s, 9H, N(CH_3)$_3$), 3.52 (s, 2H, N$-CH_2$), 3.89 (s, 2H, $SiOCH_2$), 4.15−4.52 (br, 8H, Cp). ^{13}C NMR (DMF-d_7): δ = −3.2 (Si$-CH_3$), 53.0 (N(CH_3)$_3$), 57.1, 66.5, and 67.6 (OCH_2CH_2 and *ipso*-Cp), 71.4−73.4 (Cp). Anal. Calcd for $C_{16}H_{24}FeNOSiI$: C, 41.9; H, 5.3; N, 3.1. Found: C, 41.0; H, 5.6; N, 2.8. GPC (THF, PS standards): M_n = 6.4 × 10^4 g/mol, M_w = 9.3 × 10^4 g/mol, M_w/M_n = 1.45 for the precursor [Fe(η-C_5H_4)$_2$SiMe($OCH_2CH_2NMe_2$)]$_n$.

Complex Preparation. The complexes of **PFS-(3,4,5)*n*G1** were prepared by respectively mixing the potassium salt of 3,4,5-tris(*n*-alkan-1-yloxy)benzoic acid [**(3,4,5)*n*G1-COOK**, n = 12, 14, 16] dendrons with PFS in 90% of ethanol/H_2O solution at about 75 °C

Scheme 3

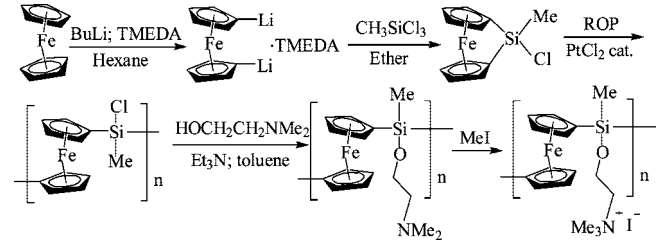

(Scheme 1). As a general procedure, 1 mmol of the dendron was dissolved in 20 mL of 90% of ethanol aqueous solution at about 75 °C and slowly added dropwise into 90% of an ethanol/water mixture containing the 1:1 stoichiometric PFS under stirring. Yellow solid precipitated in the mixture immediately, visually indicating the formation of the ionic complex between **PFS** and **(3,4,5)*n*G1-COOK**. Then, the mixture was cooled to room temperature and filtered. Finally, the yellow precipitate was washed with hot 90% of ethanol/H_2O solution and dried under vacuum for 48 h at room temperature. A strict 1:1 stoichiometric complex was obtained according to N content determined by elemental analysis.

Glassy Carbon (GC) Electrode Modification. As a general procedure, a Teflon-shrouded GC (geometric surface area 0.071 cm^2) electrode was burnished with 0.05 μm Al_2O_3 paste, and then cleaned with pure water. The GC electrode was sonicated in ethanol and doubly distilled water after polish for 30 s, respectively. Four μL solution of the **PFS-(3,4,5)*n*G1** (n = 12, 14, 16) complex in chloroform with 0.05 mol/L was spread evenly onto the freshly burnished GC electrode with a microsyringe. The coverage Γ of the complex on the electrode was estimated as 2.85 × 10^{-6} mol/cm^2 according to the 1:1 stoichiometry. In order to obtain a smooth and dense complex film, a small bottle was sealed tightly covering the electrode to serve as a closed chamber to make chloroform evaporate slowly. The GC electrode modified with the **PFS-(3,4,5)*n*G1** complex film was then dried in N_2 atmosphere.

Measurements. X-ray diffraction (XRD) of the complex powder was performed in transmission geometry with an X'pert PRO diffractometer (40 kV, 40 mA) using Cu K_α radiation (wavelength λ = 0.154 nm) at room temperature. The 2θ ranged from 1° to 30° and the scan step was 0.01° in 2θ with a counting time of 1 s/step. The differential scanning calorimetry (DSC) was carried out with 3−5 mg of sample in a 6 mm aluminum pan on a Netzsch DSC 204 under nitrogen atmosphere at heating or cooling rate of 10 °C/min following the temperature sequence as room temperature → 120 °C → −60 °C → 220 °C for the complexes. Thermogravimetry (TG) was measured with a Netzsch TG 209 under nitrogen atmosphere at heating rate of 10 °C/min starting from room temperature to 800 °C. ^{1}H NMR and ^{13}C NMR spectra were obtained on a Varian INOVA 500NB spectrometer. Molecular weight was determined by gel permeation chromatography (GPC) with a Waters apparatus at 40 °C using THF as elution and narrowly distributed polystyrene as standard. Polarized optical microscope (POM) of Zeiss Axiophot was used with a Linkam hot stage. The

Scheme 2

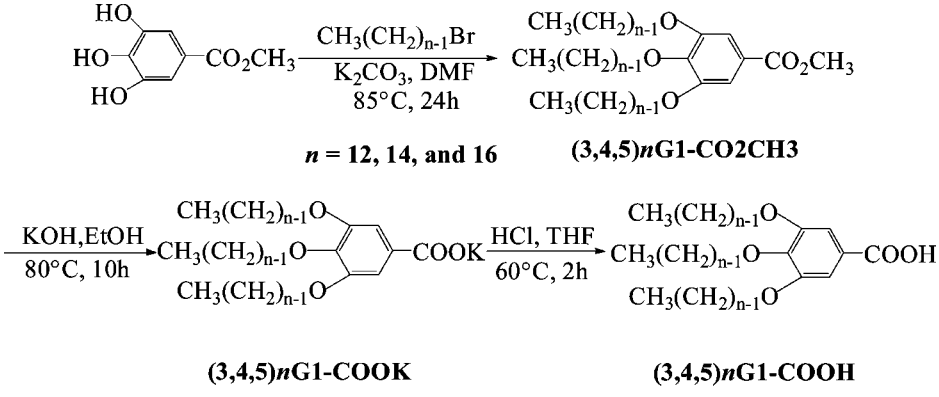

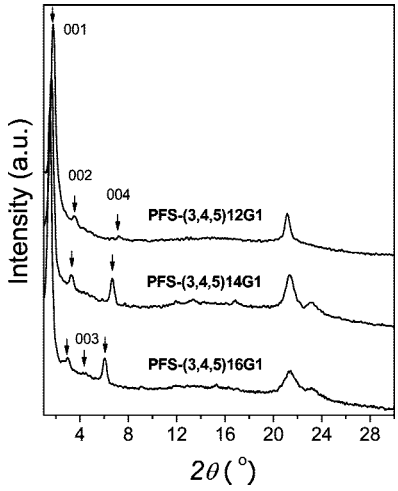

Figure 1. XRD profiles of the **PFS-(3,4,5)*n*G1** (n = 12, 14, 16) complexes at room temperature.

Table 1. X-ray Data of the Complexes PFS-(3,4,5)*n*G1 (n = 12, 14, 16)

complex	d_{001} (Å)	d_{002} (Å)	d_{003}(Å)	d_{004} (Å)	mesophase
PFS-(3,4,5)12G1	48.4	24.8		12.1	lamellar
PFS-(3,4,5)14G1	53.4	27.0		13.1	lamellar
PFS-(3,4,5)16G1	57.6	29.0	19.3	14.4	lamellar

sample was heated from room temperature to 170 °C to remove the heat history and then cooled to room temperature and subsequently heated to 170 °C again at the rate of 10 °C/min. The POM photos of the **PFS-(3,4,5)*n*G1** complexes were taken at 25 °C, 120 °C and the temperature above T_i for the crystalline phase, liquid crystalline phase, and isotropic state, respectively. Cyclic voltammogram (CV) measurements were performed on a CHI 660C electrochemical workstation (CH Instruments, Shanghai) at room temperature under nitrogen atmosphere in 0.1 M of NaCl solution using a three-electrode system. The complex film modified GC was used as the working electrode, a platinum wire as the counter electrode, and a saturated calomel as the reference electrode (SCE). The sweep range was from −0.4 V to +1.0 V versus the SCE.

3. Results and Discussion

Stacking Structure of PFS-(3,4, 5)nG1 Complexes. XRD measurements were performed to reveal the supramolecular structure of the complexes. Figure 1 depicts the XRD profiles for the three **PFS-(3,4,5)*n*G1** complexes. In the wide angle region, all complexes display one or two sharp diffractions at 2θ of 21 ∼ 24°, which indicates the presence of crystalline phase in the complexes. The three dendritic amphiphiles are crystalline while PFS is an amorphous polymer, hence, the crystalline structure of the **PFS-(3,4,5)*n*G1** complexes should come from the ionically bound dendritic amphiphiles. Recently, Manner et al. prepared a series of linear dendronized PFS polymers via the macromolecular reaction of reactive PFS-Cl and different dendrons with a focal hydroxyl group by covalent bond.[40] However, no crystalline phase was observed from these linear dendronized PFS polymers. Thus, the formation of side chain

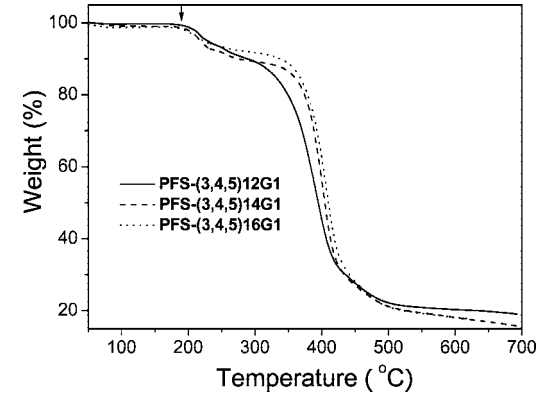

Figure 3. TG thermogram of the complexes **PFS-(3,4,5)*n*G1** (n = 12, 14, and 16).

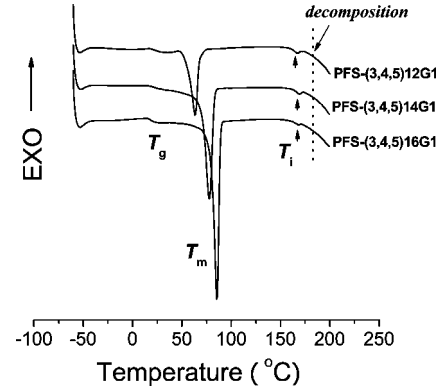

Figure 4. DSC traces of **PFS-(3,4,5)*n*G1** (n = 12, 14, and 16) recorded during the second heating run at the rate of 10 °C/min.

crystalline structure in the **PFS-(3,4,5)*n*G1** complexes seems to result from the cooperative binding of dendritic amphiphiles along the PFS main chain through the electrostatic and hydrophobic interactions in the self-assembly.

Furthermore, in the small angle region, there are at least three reflections at the equidistant positions in the d scale as 1:2:4 for the three **PFS-(3,4,5)*n*G1** complexes, indicating an ordered lamellar mesomorphous structure in the complexes at room temperature. It is noted that the strength of the 002 and 004 reflections becomes stronger with increasing n and especially the 003 reflection appears for n = 16, suggesting the formation of more ordered stacking structure in the complex with higher n. That is, the longer alkyl tail of bound dendrons improves the nanoscopic long-range order. As expected, the corresponding long period increases with n (Table 1).

Normally, surfactants are organized mainly in two different ways in the polymer-amphiphile complex: bilayer with opposite chain ends and monolayer with interdigitated alkyl tails.[9,41] The tilting of the surfactant tails is also possible in the packing structure of the complex.[42] In order to reveal the packing structure of the complex, the total length of the dendrons is estimated. Taking the **(3,4,5)16G1-COOK** as an example, the

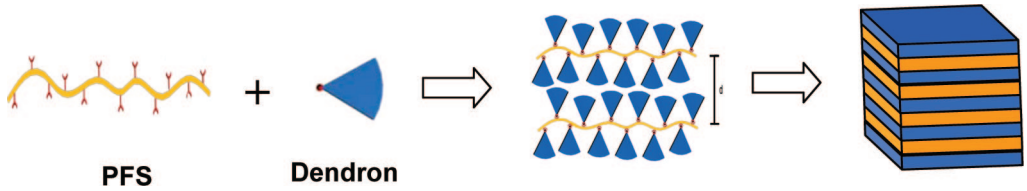

Figure 2. Stacking model for the complexes at room temperature: the end-to-end bilayer lamella mesomorphous structure for **PFS** series complexes.

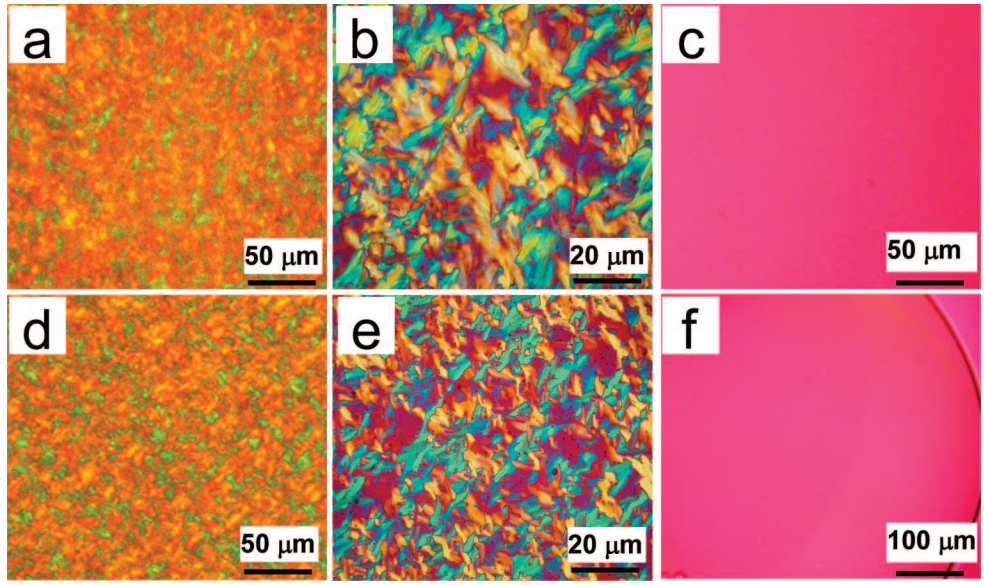

Figure 5. Polarized optical micrographs of the complexes: (a) **PFS-(3,4,5)12G1** at 25 °C, (b) **PFS-(3,4,5)12G1** at 120 °C, (c) **PFS-(3,4,5)12G1** at 170 °C, (d) **PFS-(3,4,5)16G1** at 25 °C, (e) **PFS-(3,4,5)16G1** at 120 °C, and (f) **PFS-(3,4,5)16G1** at 170 °C.

Table 2. Thermal Properties of the Complexes PFS-(3,4,5)*n*G1 (*n* = 12, 14, 16)

complex	T_g (°C)	$T_m{}^a$ (°C)	$\Delta H_m{}^b$ (J/g)	$T_i{}^a$ (°C)	$\Delta H_i{}^b$ (J/g)
PFS-(3,4,5)12G1	16.0	63.7	33.3	166.8	1.02
PFS-(3,4,5)14G1	15.2	77.6	53.9	169.4	0.89
PFS-(3,4,5)16G1	13.1	85.4	69.7	168.4	0.72

[a] DSC peak value. [b] Melting heat at the second heating run.

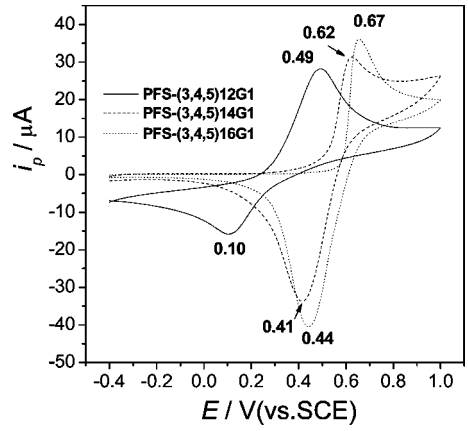

Figure 6. Cyclic voltammogram of the complexes **PFS-(3,4,5)*n*G1** (*n* = 12, 14, and 16) with scan rate of 0.1 V/s in 0.1 M of NaCl solution at 25 °C.

increment of one carbon atom in a stretched alkyl chain is about 1.25 Å and the length of a phenoxy moiety (C_6H_5-O) is about 5.3 Å.[7] Therefore, the length of **(3,4,5)16G1-COOK** should be about 25.3 Å. This value is slightly smaller than half of the long period of the complex **PFS-(3,4,5)16G1** (28.8 Å). Therefore, we deem that bound dendrons in the complex are stacked into a bilayer arrangement by taking into account the thickness of the PFS chain layer. **PFS-(3,4,5)12G1** and **PFS-(3,4,5)14G1** have the same arrangement as the **PFS-(3,4,5)16G1** according to the similar calculation. As an illustration, the stacking end-to-end bilayer lamella model for the **PFS-(3,4,5)*n*G1** complexes at room temperature are shown in Figure 2.

Thermal Properties and POM Analysis of PFS-(3,4,5)*n*G1 Complexes. In order to understand the nature of these **PFS-(3,4,5)*n*G1** complexes, we determined the thermal properties with TG and DSC. TG thermograms in Figure 3 demonstrate that there is no significant weight-loss up to 180 °C for these complexes, indicating their high thermal stability.

It is noted from Figure 4 that the **PFS-(3,4,5)*n*G1** complexes (*n* = 12, 14, and 16) have two clear endothermic transitions in the DSC curve from −60 to +220 °C. The first stronger endothermic transition belongs to the melting of the side chain crystal of ionically bound dendrons in the **PFS-(3,4,5)*n*G1** complexes. The preceding XRD diffraction profiles also support the existence of crystal phase in the complexes at room temperature. POM photos further illustrate the crystalline state texture of these complexes (Figure 5a,d). The corresponding melting point T_m (peak value) is listed in Table 2 for the **PFS-(3,4,5)*n*G1** complexes. As known from Table 2, T_m of the complexes increases from 64 to 85 °C with increasing *n*, which agrees well with the increase in melting point of the dendrons with different tail lengths.

On the other hand, a weak endothermic transition is observed above the corresponding melting temperature for each complex. We wondered whether it was the transition from ionic liquid crystal to isotropic phase. It is significant to directly observe the liquid crystal phase with a POM. As expected, POM photos at 120 °C between these two endothermic transition temperatures show that the **PFS-(3,4,5)12G1** and **PFS-(3,4,5)16G1** complexes exhibit the birefringent random polygon-like texture (Figure 5b,e). Furthermore, an isotropic phase without birefringent texture is observed from the complexes **PFS-(3,4,5)12G1** and **PFS-(3,4,5)16G1** at 170 °C above the corresponding transition T_i (Figure 5c,f). Therefore, the weak endothermic transition in DSC curve is attributed to the liquid crystal phase to isotropic transition, i.e.; **PFS-(3,4,5)*n*G1** complexes are in the liquid crystalline state of ionic thermotropic SmA between T_m and isotropic transition temperature T_i. The corresponding isotropic temperature T_i of the **PFS-(3,4,5)*n*G1** complexes increases slightly with increasing *n* (Table 2), indicating that the alkyl chain length of the dendrons has somewhat effect on T_i. The corresponding transition heat is between 0.72 to 1.02 J/g for the complexes, similar to the isotropic heat usually observed from small molecule liquid crystals.[43] To the best of our knowledge, few studies on the thermotropic side chain liquid-crystalline PFS have been reported up to now except Manners' report on liquid-crystalline PFS polymers.[37] The present study offers a simple approach to the preparation of

side chain liquid crystalline PFS polymers. The glass transition value T_g of the polymer main chain in the **PFS-(3,4,5)*n*G1** complexes observed from the DSC curve is almost independence of alkyl chain length n, considering experimental uncertainty.

Electrochemical Behavior of Complexes. Interesting property of the PFS polymers is the redox activity,[44−47] which has potential application in the fields of chemical sensor, electrocatalyst, modified electrode, etc. For this purpose, we further studied the electrochemical behavior of these complexes with CV technique in 0.1 M of NaCl solution at 25 °C. To obtain stable and reproducible CV data from the complex coated GC electrode, the successive potential sweep from −0.4 to +1.0 V (vs SCE) at scan rate of 0.1 V/s was repeated many times until approaching a steady state, i.e., the voltammetric current was no longer changed and the peak separation was kept as a constant. Figure 6 depicts the CV curves of the GC electrode modified with these complexes at a scan rate of 0.1 V/s within the potential range of −0.4 to +1.0 V. A couple of redox peaks are observed from each curve for each ionic complex, similar to the redox behavior of other PFS polymers.[44−46] The potential difference ΔE ($=E_{pa} - E_{pc}$) is 0.39, 0.21, and 0.23 V for the complex **PFS-(3,4,5)*n*G1** with $n = 12$, 14, and 16, respectively. The small potential difference ΔE indicates that the **PFS-(3,4,5)*n*G1** complexes exhibit a good redox reversibility, which offers promising applications in electrochemical sensors.

4. Conclusions

A series of novel redox-active polyelectrolyte-dendritic amphiphilic complexes **PFS-(3,4,5)*n*G1**, ($n = 12$, 14, 16) were prepared through the ionic self-assembly of the poly(ferrocenylsilane) and dendron amphiphiles. These **PFS-(3,4,5)*n*G1** complexes are in crystalline state at room temperature due to the crystallization of the dendritic amphiphilics. The ionic thermotropic liquid crystal is formed in the **PFS-(3,4,5)*n*G1** complexes above T_m. These **PFS-(3,4,5)*n*G1** complexes have a good redox reversibility, which promises to be used in electrochemical sensors. The present study offers a simple approach to fabricate side chain liquid crystal of PFS polymers.

Acknowledgment. Financial support from the NSF of China (50873037 and 20534020) and NCET is gratefully acknowledged.

References and Notes

(1) Faul, C. F. C.; Antonietti, M. *Adv. Mater.* **2003**, *15*, 673.
(2) Zhou, S.; Chu, B. *Adv. Mater.* **2000**, *12*, 545.
(3) Ikkala, O.; Brinke, G. T. *Science* **2002**, *292*, 2407.
(4) Antonietti, M.; Conrad, J.; Thünemann, A. F. *Macromolecules* **1994**, *27*, 6007.
(5) Ujiie, S.; Takagi, S.; Sato, M. *High Perform. Polym.* **1998**, *10*, 139.
(6) Macknight, W. J.; Ponomarenko, E. A.; Tirrell, D. A. *Acc. Chem. Res.* **1998**, *31*, 781.
(7) Zhou, S.; Zhao, Y.; Cai, Y.; Wang, D.; Xu, D. *Chem. Commun.* **2003**, 1932.
(8) Ober, C. K.; Wegner, G. *Adv. Mater.* **1997**, *9*, 17.
(9) Thünemann, A. F. *Prog. Polym. Sci.* **2002**, *27*, 1473.
(10) Chen, L.; Xu, S.; McBranch, D.; Whitten, D. *J. Am. Chem. Soc.* **2000**, *122*, 9302.
(11) Thünemann, A. F.; Ruppelt, D.; Schnablegger, H.; Blaul, J. *Macromolecules* **2000**, *33*, 2124.
(12) Ren, B.; Tong, Z.; Liu, X.; Wang, C.; Zeng, F. *Langmuir* **2004**, *20*, 10737.
(13) Cheng, Z.; Ren, B.; Gao, M.; Liu, X.; Tong, Z. *Macromolecules* **2007**, *40*, 7638.
(14) Antonietti, M.; Conrad, J. *Angew. Chem., Int. Ed. Engl.* **1994**, *33*, 1869.
(15) Ikkala, O.; Brinke, G. T. *Chem. Commun.* **2004**, 2131.
(16) Ren, B.; Cheng, Z.; Tong, Z.; Liu, X.; Wang, C.; Zeng, F. *Macromolecules* **2005**, *38*, 5675.
(17) Ren, B.; Cheng, Z.; Tong, Z.; Liu, X.; Wang, C.; Zeng, F. *Macromolecules* **2006**, *39*, 6552.
(18) Canilho, N.; Kasemi, E.; Schluter, A. D.; Mezzenga, R. *Macromolecules* **2007**, *40*, 2822.
(19) Caniho, N.; Scholl, M.; Klok, H. A.; Mezzenga, R. *Macromolecules* **2007**, *40*, 8374.
(20) Canilho, N.; Kasemi, E.; Schlüter, A. D.; Ruokolainen, J.; Mezzenga, R. *Macromolecules* **2007**, *40*, 7609.
(21) Martín-Rapún, R.; Marcos, M.; Omenat, A.; Barberá, J.; Romero, P.; Serrano, J. L. *J. Am. Chem. Soc.* **2005**, *127*, 7397.
(22) Smith, R. C.; Fischer, W. M.; Gin, D. L. *J. Am. Chem. Soc.* **1997**, *119*, 4093.
(23) Zhu, X.; Beginn, U.; Moller, M.; Gearba, R. I.; Anokhin, D. V.; Ivanov, D. A. *J. Am. Chem. Soc.* **2006**, *128*, 16928.
(24) Marcos, M.; Martín-Rapún, R.; Omenat, A.; Barberá, J.; Serrano, J. L. *Chem. Mater.* **2006**, *18*, 1206.
(25) Cheng, Z.; Ren, B.; Shan, H.; Liu, X.; Tong, Z. *Macromolecules* **2008**, *41*, 2656.
(26) Canilho, N.; Kasemi, E.; Mezzenga, R.; Schlüter, A. D. *J. Am. Chem. Soc.* **2006**, *128*, 13998.
(27) Thünemann, A. F.; Ruppelt, D. *Langmuir* **2000**, *16*, 3221.
(28) Power-Billard, K. N.; Manners, I. *Macromolecules* **2000**, *33*, 26.
(29) Jäkle, F.; Wang, Z.; Manners, I. *Macromol. Rapid Commun.* **2000**, *21*, 1291.
(30) Wang, Z.; Lough, A.; Manners, I. *Macromolecules* **2002**, *35*, 7669.
(31) Ginzburg, M.; Galloro, J.; Jäkle, F.; Power-Billard, K. N.; Yang, S.; Sokolov, I.; Lam, C. N. C.; Neumann, A. W.; Manners, I.; Ozin, G. A. *Langmuir* **2000**, *16*, 9609.
(32) Hempenius, M. A.; Péter, M.; Robins, N. S.; Kooij, E. S.; Vancso, G. J. *Langmuir* **2002**, *18*, 7629.
(33) Hempenius, M. A.; Robins, N. S.; Lammertink, R.G. H.; Vancso, G. J. *Macromol. Rapid Commun.* **2001**, *22*, 30.
(34) Hempenius, M. A.; Brito, F. F.; Vancso, G. J. *Macromolecules* **2003**, *36*, 6683.
(35) Hempenius, M. A.; Vancso, G. J. *Macromolecules* **2002**, *35*, 2445.
(36) Ma, Y.; Dong, W.; Kooij, E. S.; Hempenius, M. A.; Mohwald, H.; Vancso, G. J. *Soft. Matter.* **2007**, *3*, 889.
(37) Liu, X.; Bruce, D. W.; Manners, I. *J. Organomet. Chem.* **1997**, *548*, 49.
(38) Percec, V.; Holerca, M. N.; Uchida, S.; Cho, W.; Ungar, G.; Lee, Y.; Yeardley, D. J. P. *Chem.-Eur. J.* **2002**, *8*, 1106.
(39) Percec, V.; Schlueter, D.; Ronda, J. C.; Johansson, G.; Ungar, G.; Zhou, J. P. *Macromolecules* **1996**, *29*, 1464.
(40) Kim, K. T.; Han, J.; Ryu, C. Y.; Sun, F. C.; Sheiko, S. S.; Winnik, M. A.; Manners, I. *Macromolecules* **2006**, *39*, 7922.
(41) Thünemann, A. F.; General, S. *Langmuir* **2000**, *16*, 9634.
(42) Hammond, M. R.; Mezzenga, R. *Soft Matter.* **2008**, *4*, 952.
(43) Gray, G. W.; Goodby, J. W. J. *Smectic Liquid Crystals*; Leonard Hill: Glasgow, 1984; p 21.
(44) Manners, I. *Science* **2001**, *294*, 1664.
(45) Wang, X.; Wang, L.; Wang, J.; Chen, T. *J. Phys. Chem. B* **2004**, *108*, 5627.
(46) Zhao, D.; Ren, B.; Liu, S.; Liu, X.; Tong, Z. *Chem. Commun.* **2006**, 779.
(47) Ren, B.; Zhao, D.; Liu, S.; Liu, X.; Tong, Z. *Macromolecules* **2007**, *40*, 4501.

MA900207E